

Collective  $E2$  transitions of midshell Ba isotopes in the boson expansion theory

H. Sakamoto

Faculty of Engineering, Gifu University, Gifu 501-1193, Japan

(Received 29 August 2000; published 29 June 2001)

Collective  $E2$  transitions of midshell Ba isotopes are studied by means of the boson expansion theory. The fermion Hamiltonian is comprised of the self-consistent  $QQ$  interaction with higher-order (many-body) terms, monopole- and quadrupole-pairing interactions in addition to the spherical limit of the Nilsson Hamiltonian. The Kishimoto-Tamura method of normal-ordered linked-cluster expansion of the modified Marumori boson mapping is applied to construct the microscopic boson image of the Hamiltonian and that of the  $E2$  operator. It is shown that the marked increase of quadrupole collectivity, indicated by the enhancement of experimental  $B(E2)$ , as neutron numbers approach the midshell value of  $N=66$  can be reproduced naturally in terms of the microscopic boson expansion theory by using a standard value of the effective charge.

DOI: 10.1103/PhysRevC.64.024303

PACS number(s): 21.60.Ev, 27.60.+j

## I. INTRODUCTION

Enlargement of the  $B(E2;2_1^+ \rightarrow 0_1^+)$  values is one of the fundamental indices of the enhanced quadrupole collectivity in even-even nuclei. These  $B(E2)$  values are often used most importantly to deduce the experimental deformation of the nuclear ground state. The experimental  $B(E2;2_1^+ \rightarrow 0_1^+)$  values of the rare-earth nuclei in the  $50 \leq Z \leq 82$ ,  $82 \leq N \leq 126$  region are known to peak at (or very close to) midshell, while whether a similar behavior occurs in the  $50 \leq (Z, N) \leq 82$  region has been an open and challenging problem from both experimental and theoretical viewpoint [1].

About a decade ago, a possible ‘‘saturation’’ of the  $B(E2;2_1^+ \rightarrow 0_1^+)$  values in the midshell ( $N=66$ ) region was once suggested experimentally, and a systematic calculation of the collective states in the Xe-Ba-Ce region was made within the proton-neutron interacting boson model (IBM-2). Then it was concluded that the Pauli blocking factors in the IBM-2 are of particular importance to obtain the ‘‘saturation’’ of the  $B(E2)$  in the midshell region [2].

Afterward, however, Walpe *et al.* reported new data of the lifetime for the  $2_1^+ \rightarrow 0_1^+$  transition in  $^{120}\text{Xe}$ , which was more than a factor of 2 lower than the previously adopted value. The data suggested a disappearance of the ‘‘saturation’’ effect and a significant discrepancy between experimental values and the IBM-2 calculations *with* the Pauli blocking factors [3]. Then Raman *et al.* reported a revised compilation of experimental data including several additional modern experiments and concluded that the measured  $B(E2;2_1^+ \rightarrow 0_1^+)$  values for the light Xe isotopes show a marked increase in the midshell region [1].

Recently, also for the light Ba isotopes, several modern experimental data have been accumulated and the similar trend as above for the  $B(E2)$  in this region has been ascertained [4–13]. In Ref. [5], Uchiyama *et al.* reported that the revised systematic trend of  $B(E2)$  values for even Ba isotopes from  $^{124}\text{Ba}$  to  $^{136}\text{Ba}$  is well reproduced by the IBM-2 calculations *without* the Pauli blocking factors, which seems rather ironical considering the microscopic origin of the IBM.

Thus, as stated in Ref. [1], providing a consistent expla-

nation for the systematics of the experimental  $B(E2;2_1^+ \rightarrow 0_1^+)$  values in this midshell region without any concomitant change in the energies of the low-lying states, is an important challenge facing nuclear models. The purpose of this paper is to report briefly some results of our recent investigation on the quadrupole collective properties of  $^{122-136}\text{Ba}$  by means of the boson expansion theory (BET).

The BET is known to be a very promising method for the description of anharmonicities in nuclear quadrupole collective motions, if couplings to noncollective states are faithfully included in the calculation [14,15]. The present formalism is based on the Kishimoto-Tamura method of the normal-ordered linked-cluster expansion of the modified Marumori boson mapping [16] (referred to as KT-3), in which boson operators are allowed to act upon the ideal-boson states. Numerical calculations are performed by using many useful techniques reported in Refs. [14,15] with several refinements developed in our previous works [17–19].

## II. MODEL HAMILTONIAN

The model Hamiltonian with which we start is given in fermion operators as

$$H = h_{sp} + (H_{0-pair} - \lambda \hat{N}) + H_{2-pair} + V^{(2)} + V^{(3)} + V^{(4)} \quad (1)$$

with

$$h_{sp} = \sum_{i=1}^A \left[ \frac{p^2}{2m} + \frac{m}{2} \hat{\omega}^2 r^2 - \kappa \hbar \hat{\omega} \{2(\mathbf{1} \cdot \mathbf{s}) + \mu(\mathbf{I}^2 - \langle \mathbf{I}^2 \rangle)\} \right]_i, \quad (2)$$

$$H_{0-pair} = -\frac{G_0}{4} \hat{P}_0^\dagger \hat{P}_0, \quad (3)$$

$$H_{2-pair} = -\frac{G_2}{2} (\hat{P}_2^\dagger \cdot \hat{P}_2), \quad (4)$$

$$V^{(2)} = -\frac{\chi^{(2)}}{2}(\hat{Q}_2 \cdot \hat{Q}_2), \quad (5)$$

$$V^{(3)} = -\frac{\chi^{(3)}}{3!}[\sqrt{56\pi/5}(\hat{Q}_2 \hat{Q}_2 \hat{Q}_2) - 3\hat{R}_0(\hat{Q}_2 \cdot \hat{Q}_2)], \quad (6)$$

$$V^{(4)} = -\frac{\chi^{(4)}}{4!} \left[ \frac{48\pi}{5}(\hat{Q}_2 \cdot \hat{Q}_2)^2 - 8\sqrt{56\pi/5}\hat{R}_0(\hat{Q}_2 \hat{Q}_2 \hat{Q}_2) + 12\hat{R}_0^2(\hat{Q}_2 \cdot \hat{Q}_2) \right]. \quad (7)$$

Here  $h_{sp}$  is the spherical limit of the Nilsson Hamiltonian, and the values of  $\kappa$ ,  $\mu$ , and  $\hat{\omega}$  are fixed in accordance with the systematics [20]

$$\begin{aligned} \mu_n &= 0.624 - 1.234 \frac{A}{1000}, & \kappa_n &= 0.0641 - 0.0026 \frac{A}{1000}, \\ \mu_p &= 0.493 + 0.649 \frac{A}{1000}, & \kappa_p &= 0.0766 - 0.0779 \frac{A}{1000}, \\ \hat{\omega}_{n,p} &= \hat{\omega} \left( 1 \pm \frac{N-Z}{3A} \right), & \hbar \hat{\omega} &= 41A^{-1/3} \text{ (MeV)}, \end{aligned} \quad (8)$$

and our fermion model space is spanned by  $2p_{1/2}$ ,  $2p_{3/2}$ ,  $1f_{5/2}$ ,  $3s_{1/2}$ ,  $2d_{3/2}$ ,  $2d_{5/2}$ ,  $1g_{7/2}$ ,  $1g_{9/2}$ , and  $1h_{11/2}$  orbits for protons and  $3s_{1/2}$ ,  $2d_{3/2}$ ,  $2d_{5/2}$ ,  $1g_{7/2}$ ,  $2f_{7/2}$ ,  $1h_{9/2}$ ,  $1h_{11/2}$ , and  $1i_{13/2}$  orbits for neutrons. As for the Nilsson parameters  $\kappa$  and  $\mu$ , there are relatively recent parameters, e.g. those proposed in Refs. [21,22]. If we use these parameters, however, in principle, we must reexamine the self-consistency between the one-body field and the effective interactions because these parameters possess complicated velocity dependences or density dependences. To avoid this complexity, we adopted the simple and standard parameter set of Ref. [20] in the present work.

In the above Hamiltonian,  $H_{0-pair}$  and  $H_{2-pair}$  are monopole- and quadrupole-pairing interactions,  $V^{(2)}$  is the ordinary two-body  $QQ$  interaction, while  $V^{(3)}$  and  $V^{(4)}$  are the effective three- and four-body interactions introduced as the higher-order terms of the  $QQ$  interaction to recover the *nuclear self-consistency* (the nuclear saturation and the self-consistency [23,24]) in higher-order accuracy especially when more than one mode is simultaneously excited in a system [25–27]. Essentially the same type of many-body interactions was derived by Marshalek [28], and the three-body interaction has been applied to the analysis of anharmonic  $\gamma$  vibrations in  $^{168}\text{Er}$  by Matsuo and Matsuyanagi [29] and Stotts and Tamura [30], to the analysis of two-phonon states in Ru and Se isotopes by Aiba [31], and to the analysis of shape transition in Sm isotopes by Yamada [32].

The origin of the quadrupole-pairing interaction with its self-consistent coupling strength has been discussed in connection with the *local Galilean invariance* of the system under the quadrupole collective motion in the presence of the monopole-pairing interaction [33,34].

The strengths of the monopole-pairing interactions,  $G_0(p)$  for protons and  $G_0(n)$  for neutrons, are fixed to fit the experimental gap energies through the gap equations, where the gap parameters are derived from the atomic mass evaluation compiled by Audi and Wapstra [35]. The strengths of the self-consistent  $QQ$  interaction and its higher-order terms are parametrized as

$$f_2 = \chi^{(2)}/\chi_2^{self} = \chi^{(3)}/\chi_3^{self} = \chi^{(4)}/\chi_4^{self}, \quad (9)$$

where  $\chi_2^{self}$ ,  $\chi_3^{self}$ , and  $\chi_4^{self}$  are the self-consistent values of  $\chi^{(2)}$ ,  $\chi^{(3)}$ , and  $\chi^{(4)}$ , respectively, which are derived in Ref. [27]. For the strengths of the quadrupole-pairing interactions,  $G_2(p)$  for protons and  $G_2(n)$  for neutrons, we parametrize them as

$$g'_2 = G_2(p)/G_2^{self}(p) = G_2(n)/G_2^{self}(n), \quad (10)$$

where  $G_2^{self}(p)$  and  $G_2^{self}(n)$  are the self-consistent strengths of the quadrupole-pairing interaction for protons and neutrons, respectively [34]. These parametrizations are introduced to reduce the number of free parameters. In calculating the energy spectra, the above two dimensionless parameters,  $f_2$  and  $g'_2$ , are varied slightly around the vicinity of the predicted value, i.e., unity.

### III. BOSON EXPANSION

In the KT-3 formalism of BET, a truncated fermion space  $T_F$  is mapped onto a corresponding subspace  $T$  in the ideal boson space. The one-to-one correspondence between a fermion state in the truncated space and a boson state is realized as

$$|n:t\rangle = U|n:t\rangle, \quad |n:t\rangle = U^\dagger|n:t\rangle, \quad (11)$$

with

$$U = \sum_{(n:t)} |n:t\rangle\langle n:t|, \quad (12)$$

where  $|n:t\rangle$  is the orthonormalized fermion state with  $n$  Tamm-Dancoff (TD) phonons (correlated quasiparticle pairs),  $|n:t\rangle$  is the ideal- $n$ -boson state, and  $t$  represents a set of all the other quantum numbers necessary to distinguish different states in the each subspace. A boson image  $(O_F)_B$  of a fermion operator  $O_F$  is defined by

$$(O_F)_B \equiv U O_F U^\dagger \quad (13)$$

so as to satisfy

$$\langle m:t|O_F|n:t'\rangle = \langle m:t|(O_F)_B|n:t'\rangle \quad (14)$$

in the truncated subspace.

In the presence of the superconducting correlation, to remove spurious modes associated with particle number non-conservation, we use the prescription developed in Refs.

[17,19]. In that case, all the  $|n:t\rangle$  in the above equations are replaced by  $|\overline{n:t}\rangle$ , the orthonormalized *physical* fermion state, where the spurious modes are approximately projected out. Detailed definitions, notations, and constructions of these quantities are given in Ref. [19].

In order to include approximately the coupling effects between relevant and irrelevant degrees of freedom, the truncated boson space  $T$  is divided into two parts, i.e.,  $P$  space and  $Q$  space. Since we are interested in the quadrupole collective motions, the space spanned only by the coherent quadrupole TD mode is identified as the  $P$  space (collective space), and its complement corresponds to the  $Q$  space (non-collective space). In the present calculations, all the possible noncollective boson states ( $I^\pi = 0^+ - 4^+$ ) that can couple directly to the states with one or two collective phonons are included. For the practical purpose, however, the space truncation is performed so that the  $Q$  space is spanned by only those noncollective states in which none of the noncollective bosons excites more than once although the collective boson may excite multiply. Then, along the line of the Feshbach formalism [36] and the perturbation theory for a quasidegenerate system [26,37–40], we can construct effective operators to be used in the  $P$  space.

The KT-3 formalism of BET is expressed in terms of the so-called  $A$  bosons, which correspond to the boson images of the TD fermion operators in the lowest order. In applications to realistic nuclei, to include the RPA-type correlations at the early stage of the calculation for the collective branch, we transform collective  $A$  bosons to new type of collective bosons, the so-called  $\alpha$  bosons, defined by

$$A^\dagger = \psi\alpha^\dagger + \phi\tilde{\alpha}, \quad \tilde{A} = \phi\alpha^\dagger + \psi\tilde{\alpha}, \quad (15)$$

with

$$\psi = \frac{1}{2}(z + z^{-1}), \quad \phi = \frac{1}{2}(z - z^{-1}). \quad (16)$$

This procedure ensures the elimination of the dangerous terms in the boson Hamiltonian and the parameter  $z$  is determined accordingly [15].

Thus, by applying the above formalism, we can obtain microscopic boson images of fermion operators, renormalized by including the noncollective coupling effects and expressed entirely in terms of the  $\alpha$  bosons. In the present analysis, we expand the Hamiltonian and the E2 operators up to fourth and third order of the bosons, respectively.

As a result, the collective Hamiltonian, i.e., the effective Hamiltonian to be used in the  $P$  space, is expressed in a compact form as

$$H_{coll} \equiv H_{PP}^{eff} = U_0 + \sum_{mni} h_{mni} H_{mni}^{(\alpha)}, \quad (17)$$

$$h_{mni} \equiv h_{mni}^{(\alpha)} + h_{mni}^{(\alpha)'}. \quad (17)$$

Here  $H_{mni}^{(\alpha)}$  are operators of the form  $(\alpha^\dagger)^m (\tilde{\alpha})^n$  and the additional index  $i$  distinguishes terms that have the same  $m$  and  $n$ . They are expressed as

$$\begin{aligned} H_{11}^{(\alpha)} &= (\alpha^\dagger \cdot \alpha), \\ H_{20}^{(\alpha)} &= (\alpha^\dagger \cdot \alpha^\dagger) + (\alpha \cdot \alpha), \\ H_{21}^{(\alpha)} &= ([\alpha^\dagger \alpha^\dagger] \cdot \alpha) + (\alpha^\dagger \cdot [\alpha \alpha]), \\ H_{30}^{(\alpha)} &= ([\alpha^\dagger \alpha^\dagger] \cdot \alpha^\dagger) + (\alpha \cdot [\alpha \alpha]), \\ H_{22P}^{(\alpha)} &= (\alpha^\dagger \alpha^\dagger)(\alpha \alpha), \\ H_{22N}^{(\alpha)} &= (\alpha^\dagger \alpha) \{ (\alpha^\dagger \alpha) - 1 \}, \\ H_{22J}^{(\alpha)} &= \hat{J}^2 - 6(\alpha^\dagger \alpha), \\ H_{31}^{(\alpha)} &= (\alpha^\dagger \alpha^\dagger)(\alpha^\dagger \alpha) + (\alpha^\dagger \alpha)(\alpha \alpha), \\ H_{40}^{(\alpha)} &= (\alpha^\dagger \alpha^\dagger)(\alpha^\dagger \alpha^\dagger) + (\alpha \alpha)(\alpha \alpha), \end{aligned} \quad (18)$$

with

$$\hat{J}^2 \equiv -10([\alpha^\dagger \alpha]^{(1)}[\alpha^\dagger \alpha]^{(1)}). \quad (19)$$

The coefficients  $h_{mni}^{(\alpha)}$  come directly from the purely collective channels, while  $h_{mni}^{(\alpha)'}$  are the contributions from the non-collective couplings. Detailed derivations and explicit expressions of these coefficients are given in Refs. [15,17–19]. Once we obtain the collective Hamiltonian expressed by the  $\alpha$  bosons, we can calculate the eigenenergies of the collective states by diagonalizing it in the  $P$  space.

To visualize the physical properties described by the collective Hamiltonian, we transform the  $\alpha$  bosons into momenta and conjugate coordinates defined by

$$\begin{aligned} \alpha^\dagger &= \frac{1}{\sqrt{2}}(z^{-1}\beta_{2\mu} - iz\pi_{2\mu}), \\ \alpha &= \frac{1}{\sqrt{2}}(z^{-1}\beta_{2\mu} + iz\pi_{2\mu}). \end{aligned} \quad (20)$$

Then the collective Hamiltonian becomes

$$H_{coll} = T(\beta_{2\mu}, \pi_{2\mu}) + V(\beta_{2\mu}) + c_0, \quad (21)$$

where the generalized kinetic energy is given by

$$\begin{aligned} T(\beta_{2\mu}, \pi_{2\mu}) &= a_2 \pi^2 + a_4 \pi^4 \\ &\quad + b_3([\pi\beta]^{(2)} \cdot \pi) + b_4^{(1)}(\pi^2 \beta^2 + \beta^2 \pi^2) \\ &\quad + b_4^{(2)}(\beta \cdot \pi)(\pi \cdot \beta) \\ &\quad + b_4^{(3)}([\beta\pi]^{(1)} \cdot [\pi\beta]^{(1)}), \end{aligned} \quad (22)$$

while the potential energy term is expressed as

$$V(\beta_{2\mu}) \equiv V(\beta, \gamma) = c_2 \beta^2 + c_3 \beta^3 \cos 3\gamma + c_4 \beta^4, \quad (23)$$

with the intrinsic deformation parameters defined by

$$\beta_{20} = \beta \cos \gamma, \quad \beta_{2\pm 1} = 0, \quad \beta_{2\pm 2} = \sqrt{\frac{1}{2}} \beta \sin \gamma. \quad (24)$$

TABLE I. Values of dimensionless parameter  $z$ , Hamiltonian coefficients  $h_{mni}$ , and corresponding kinetic and potential coefficients  $a$ 's,  $b$ 's, and  $c$ 's for barium isotopes calculated in the present work. Units are listed in the second column.

		$^{120}\text{Ba}$	$^{122}\text{Ba}$	$^{124}\text{Ba}$	$^{126}\text{Ba}$	$^{128}\text{Ba}$	$^{130}\text{Ba}$	$^{132}\text{Ba}$	$^{134}\text{Ba}$	$^{136}\text{Ba}$
$z$		1.892	2.162	1.976	1.838	1.762	1.643	1.491	1.450	1.255
$h_{11}$	$10^{-1}$ MeV	3.345	2.752	2.627	3.680	3.917	4.208	5.193	6.095	8.327
$h_{20}$	$10^{-6}$ MeV	3.934	1.907	-5.961	0.238	5.662	3.099	-2.235	-0.775	1.527
$h_{21}$	$10^{-1}$ MeV	2.040	-0.122	-0.136	-0.004	-0.130	-0.221	-0.415	-0.475	0.139
$h_{30}$	$10^{-2}$ MeV	4.308	-1.926	-2.051	-1.569	-1.908	-1.782	-1.809	-1.795	-1.033
$h_{22P}$	$10^{-1}$ MeV	1.510	2.452	2.831	2.708	2.379	1.462	0.685	0.362	0.198
$h_{22N}$	$10^{-1}$ MeV	3.381	5.134	5.852	5.456	4.756	2.846	1.065	0.226	0.038
$h_{22J}$	$10^{-3}$ MeV	4.348	4.156	5.688	6.605	6.831	6.419	7.222	7.810	5.726
$h_{31}$	$10^{-1}$ MeV	3.248	5.040	5.727	5.348	4.654	2.804	1.156	0.430	0.244
$h_{40}$	$10^{-1}$ MeV	0.782	1.235	1.371	1.247	1.067	0.626	0.248	0.100	0.048
$c_0$	$10^0$ MeV	2.220	3.878	4.493	3.819	3.131	1.403	-0.375	-1.310	-2.027
$c_2$	$10^2$ MeV	-1.119	-1.448	-1.919	-2.053	-2.028	-1.416	-0.575	0.032	0.530
$c_3$	$10^1$ MeV	-3.509	0.327	0.440	0.260	0.636	1.063	2.375	3.310	-0.349
$c_4$	$10^3$ MeV	0.878	0.900	1.365	1.722	1.964	1.748	1.223	0.608	0.718
$a_2$	$10^{-3}$ MeV	2.417	2.459	1.639	2.262	2.145	2.180	2.455	2.699	2.422
$b_3$	$10^{-3}$ MeV	7.325	4.954	4.853	4.384	3.878	2.491	0.890	0.407	2.321
$b_4^{(1)}$	$10^{-3}$ MeV	8.345	5.288	6.984	6.316	6.102	3.293	-2.902	-8.394	-6.386
$b_4^{(2)}$	$10^{-2}$ MeV	-0.632	-0.182	0.895	2.137	2.456	2.108	1.878	1.622	1.021
$b_4^{(3)}$	$10^{-2}$ MeV	-4.474	-4.156	-5.687	-6.605	-6.831	-6.419	-7.222	-7.810	-5.726
$a_4$	$10^{-7}$ MeV	-3.906	-3.472	-3.093	-2.887	-2.350	-1.917	-1.506	-1.215	-1.125

To relate our microscopic  $\beta_{2\mu}$  with the deformation parameters of the Bohr-Mottelson model [41,42], a scaling factor  $\xi$  is inevitably introduced as  $\beta \rightarrow \xi\beta$ ,  $\pi \rightarrow \pi/\xi$ . The determination of  $\xi$  is explained in Refs. [15,18,19]. The form of  $T(\beta_{2\mu}, \pi_{2\mu})$  cannot be given uniquely, because of the non-commutativity between  $\beta_{2\mu}$  and  $\pi_{2\mu}$ , although the sum  $T(\beta_{2\mu}, \pi_{2\mu}) + c_0$  is unique [15].

It is interesting to compare our boson Hamiltonian with the collective Hamiltonian of the generalized collective model (GCM). In Ref. [12], Petkov *et al.* applied the GCM to the Ba isotopes with  $A=124-132$ . In that case, the kinetic part of the GCM Hamiltonian is comprised only of second-order terms of  $\pi$ , while the potential part of it is considered up to the sixth-order terms of  $\beta$ , and there are eight adjustable coefficients in their total Hamiltonian. On the other hand, since the mapped Hamiltonian is expanded up to the fourth-order of boson in the present work, the kinetic part of our boson Hamiltonian contains up to the fourth-order terms of  $\pi$ , though the potential part of it contains at most fourth-order terms of  $\beta$ , and all the coefficients in our total Hamiltonian are determined as functions of  $f_2$  and  $g_2'$ , which are the only two adjustable parameters in our model Hamiltonian.

We should notice that a strong correlation between the potential energy surface and the energy spectrum holds only under the condition that all the anharmonic terms in  $T(\beta_{2\mu}, \pi_{2\mu})$  are sufficiently small. If such a condition is not met and a generalized collective mass depends crucially on coordinates, then to predict the spectrum from the shape of the potential surface only can be dangerous [15,19]. In the boson expansion approach, the adiabatic assumption is not made and generally there appear terms that are in higher

power in  $\pi$ . Such terms give corrections to the theories based on the adiabatic assumption.

#### IV. RESULTS AND DISCUSSIONS

As explained in Sec. II, we introduced two dimensionless parameters,  $f_2$  and  $g_2'$ , which measure the microscopic interactions between nucleons in nuclei. To obtain a good description of the experimental level scheme, in the present analysis, they are allowed to vary slightly around the vicinity of the predicted value, i.e., unity, for individual nuclei.

The values of dimensionless parameter  $z$ , Hamiltonian coefficients  $h_{mni}$ , and corresponding kinetic and potential coefficients  $a$ 's,  $b$ 's, and  $c$ 's calculated in the present work are summarized in Table I. The deviation of  $z$  from the unity represents how important the RPA-type of ground-state correlations and to what extent the  $\alpha$  bosons are far from the  $A$  bosons. We can verify that the ground-state correlations peak at the midshell also in this mass region. Note that  $h_{20}$  vanishes here and indeed the dangerous terms are eliminated.

The coefficients  $h_{mni} > 0$  for  $m+n > 2$  express the correlations beyond RPA. We normally have  $h_{mni} > 0$  for  $m+n = 4$ , and therefore  $c_4 > 0$ , which is necessary to prevent the nucleus from collapsing into an infinitely large deformation [15]. If  $c_2 < 0$ , the spherically symmetric shape is unstable, and in that case if  $c_3 < 0 (> 0)$ , a prolate (oblate) deformation is favored. In the present work, the values of  $c_3$  become rather small reflecting the  $\gamma$ -unstable nature of the region under consideration.

A stronger dependence of the inertial functions on deformation has been suggested by Pomorski *et al.* [43] for rare-earth nuclei. In their expression for the collective kinetic

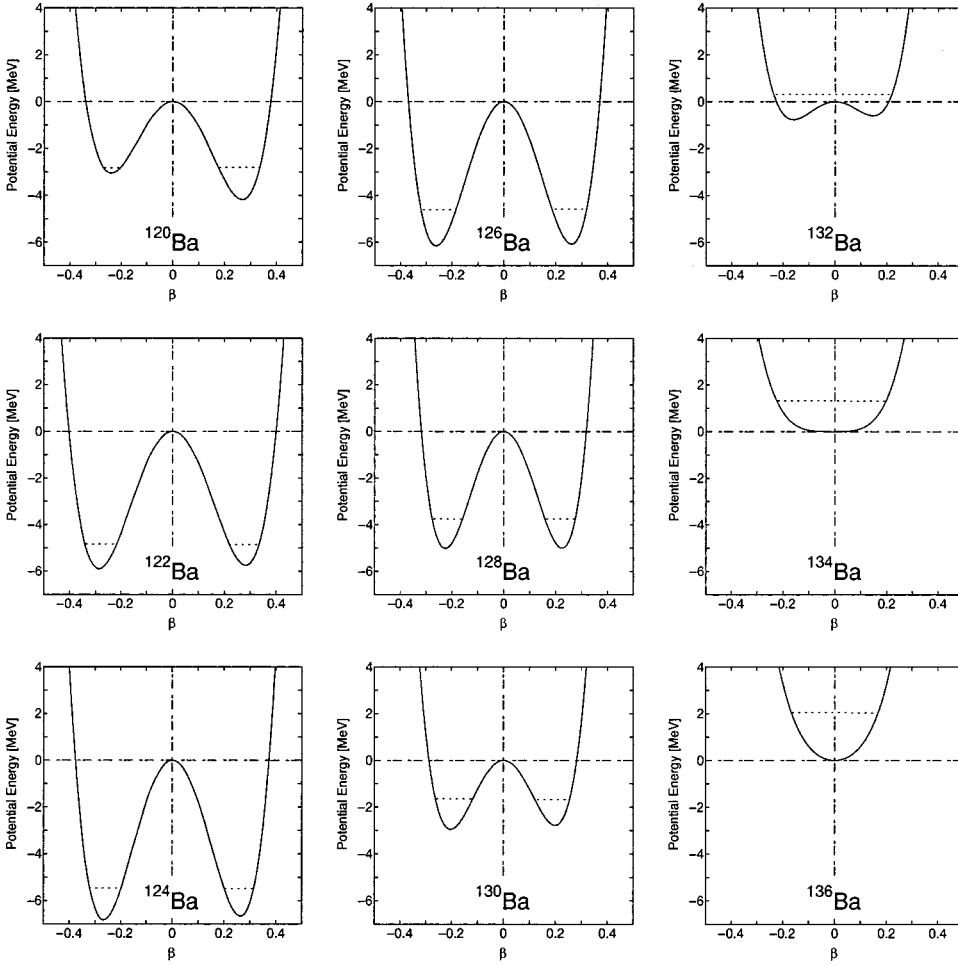


FIG. 1. Calculated potential energy surfaces for even-even barium isotopes. The horizontal dot lines indicate the calculated ground-state energy.

energy [Eq. (2.5) of Ref. [43]], the coefficient  $p$ 's are scalar functions of the collective coordinates, and contributions from higher-order terms of the coordinates are included also through these coefficients. While in Eq. (22) of the present work, where operators and coefficients are completely separated out, the coordinates  $\beta_{2\mu}$  and conjugate momenta  $\pi_{2\mu}$  are treated on the same footing and are considered up to the same order. Thus the relation between the two expressions is not so simple.

In our expression, the coefficients  $b$ 's can be interpreted as arising from the dependence of the inertial functions on deformation. As is known from Table I, the effects of such dependence are rather sensible. In Ref. [18], we discussed to a certain extent the effect of such dependence by trying to adjust the third-order mass coefficient  $b_3$  without changing the values of all the other kinetic and potential coefficients, and found that even a set of very little variations of coefficients  $h_{21}$  and  $h_{30}$  can sometimes produce significant difference in  $b_3$  and drastic change in the final level scheme, while keeping the shape of the potential surface unchanged. Thus it is very important to have a proper deformation dependence of the mass coefficients microscopically. For that purpose, we have been investigating the self-consistent velocity dependent effective interactions, e.g., the origin and the deformation dependence of the multipole pairing interactions [34,44], requiring that the velocity dependence of potentials

and that of effective interactions, both affect the mass coefficients, should be self-consistent with each other. However, probably there is still room for improving the collective mass parameters in our microscopic model.

The nonadiabatic term  $\pi^4$  considered in this paper has to be interpreted as arising from a velocity-dependent mass parameter of the collective motion. In the framework of the time-dependent perturbation theory, such terms appear in the general cranking formula as fourth-order terms of perturbation about couplings between single particles and collective velocity fields [45]. Looking at the values of  $a_4$ , the velocity dependences of the collective mass parameters do not seem so large in the present results.

Figure 1 shows the theoretical potential energy surfaces for  $^{120-136}\text{Ba}$  obtained by the present two-parameter analysis. The calculated potential energy surfaces of the Ba isotopes studied show  $\gamma$ -soft features, and such features are especially enhanced for  $^{122-130}\text{Ba}$ . In fact, we see in Fig. 1 that the difference in energy between the two potential minima are rather small compared to the zero-point energy for these nuclei.

In Fig. 2, the theoretical excitation energies in the ground-state band and those in the quasi- $\gamma$  band are plotted as a function of neutron number  $N$  and are compared with experiment. The theoretical spectra reproduce very roughly the general trends of experimental spectra, though the tendency

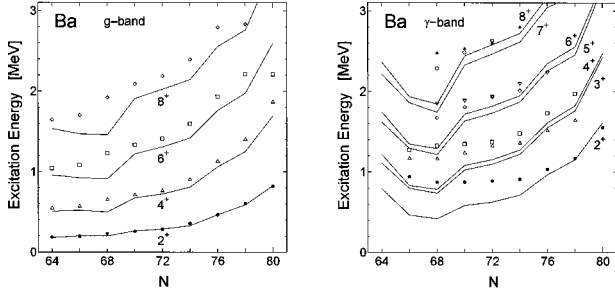


FIG. 2. Calculated and experimental excitation energies in the ground-state band (left panel) and the quasi-gamma band (right panel) of even-even barium isotopes plotted as a function of neutron number  $N$ .

to the bunching of levels in the quasi- $\gamma$  band that is characteristic to  $\gamma$  instability is too prominent in the theoretical result. A similar difficulty was observed in Refs. [15,18,19]. The calculated excitation energy of the  $2^+_{\gamma}$  state is too low compared to the experiment for isotopes with  $N \leq 74$ .

For the effects of the higher-order interactions, we can verify from the order estimation of the coupling strengths that the contributions from the four-body interaction are almost negligible while the effects of the three-body interaction are visible in this mass region. Though the effects are not always so large, excitation energies of the states in the quasi- $\gamma$  band are relatively lowered while those in the quasi- $\beta$  band are raised due to the three-body interaction. Such effects can be consistently understood from the relation between the higher-order interactions and the doubly-stretched quadrupole interaction [19], but are disadvantageous for the present specific problem of the position of the  $\gamma$  head energies.

However, as generally observed in the RPA calculation of vibrational states in deformed nuclei, the positions of the band heads are very sensitive to the choice of the single-particle energies. Therefore the difficulty in the band head energy is not always so serious but sometimes can be remedied by a proper choice of the single-particle energies. For example, we can raise slightly the position of the  $2^+_{\gamma}$  state by shifting the intruder proton  $h_{11/2}$  state upward without changing the order of the single-particle levels [18,46].

In calculating the electromagnetic properties, the quadrupole effective charge  $e_{eff}$  is introduced as the only parameter to fit the experimental data. The need for the effective charge in our calculations comes mainly due to the omission of the  $\Delta N=2$  quadrupole matrix elements, which we did intentionally, along the line of Ref. [15], to reduce the dependence on the choice of the single-particle space. It is possible to take into account the  $\Delta N=2$  matrix elements disregarded in the paper for computing reasons. However, under the presence of the pairing interactions, it is not possible to include completely matrix elements connecting different major shells even if we further enlarge the single-particle model space. As we have to truncate the model space one way or another, some  $\Delta N=2$  matrix elements are neglected to a certain extent and usually it is necessary to introduce effective charges for transition operators as well as for interaction operators. In such a situation, theoretical reference values of effective

charges inevitably become ambiguous depending on the choice of the model space.

Since the purposes of the present work is to study whether the marked increase of quadrupole collectivity as neutron numbers approach the midshell value of  $N=66$  can be reproduced naturally or not in terms of the microscopic BET by using a standard value of the effective charge, we need to remove such ambiguities and to know in advance the theoretical reference values of the effective charges for transition operators as well as for interaction operators. By cutting off the  $\Delta N=2$  quadrupole matrix elements completely, we can refer to the theoretical value of  $e_{eff}^{(int)}=1$  for the quadrupole interaction operator and the value of  $e_{eff}^{(E2)}=Z/A$  for the  $E2$  transition operator as explained transparently by Mottelson [23]. In the present analysis, to reduce the number of free parameters a common  $E2$  effective charge is adopted for both protons and neutrons, and to investigate the systematics a uniform value of it is used for all the Ba isotopes considered.

In Fig. 3 theoretical reduced transition probabilities from the first excited  $2^+$  state to the ground state of even-even barium isotopes are plotted as a function of neutron number  $N$ . Here, to give an idea of the sensitivity of the results upon the choice of the effective charge, the results for three cases,  $e_{eff}=0.50, 0.55,$  and  $0.60$ , are presented and are compared with experiment. We see that the experimental trend can be well reproduced by the present calculation with a rather standard value of effective charge, and the theoretical  $B(E2; 2^+_1 \rightarrow 0^+_1)$  value peaks at the neutron midshell also for the Ba isotopes, though the experimental data are still missing for  $^{120}\text{Ba}$ .

In Fig. 4, calculated  $B(E2; I \rightarrow I-2)$  reduced transition probabilities in the ground-state band of Ba isotopes are presented for the case of  $e_{eff}=0.55$ . Here, the first three panels show the results for  $^{124-128}\text{Ba}$  with experimental data, and the final panel provides the theoretical systematics for all the Ba isotopes considered. It is interesting to see that promising agreements between the theory and the experiment are ob-

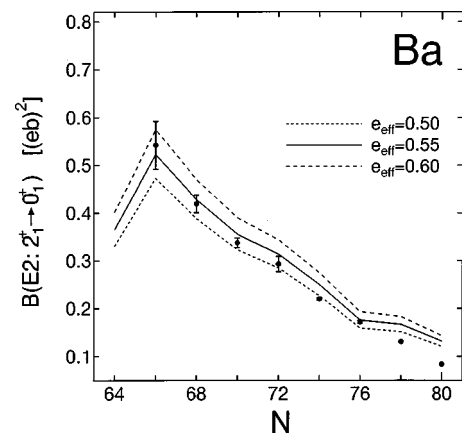


FIG. 3. The reduced transition probability from the first excited  $2^+$  state to the ground state of even-even barium isotopes plotted as a function of neutron number  $N$ . Experimental data are taken from  $^{122}\text{Ba}$  [4],  $^{124}\text{Ba}$  [5],  $^{126}\text{Ba}$  [6],  $^{128}\text{Ba}$  [7],  $^{130}\text{Ba}$  [8],  $^{132}\text{Ba}$  [9],  $^{134}\text{Ba}$  [10], and  $^{136}\text{Ba}$  [11].

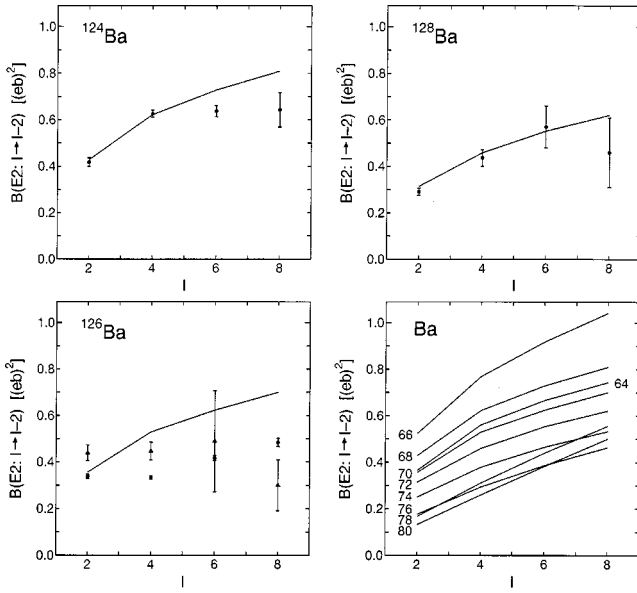


FIG. 4. Calculated and experimental  $B(E2)$  reduced transition probabilities in the ground-state band of  $^{124-128}\text{Ba}$ . In the final panel, the theoretical systematics is also shown as a function of neutron number  $N$ . Experimental data are taken from  $^{124}\text{Ba}$  [5,12],  $^{126}\text{Ba}$  [6,13], and  $^{128}\text{Ba}$  [7].

tained not only for the  $B(E2; 2_1^+ \rightarrow 0_1^+)$  but also for several other  $B(E2)$  transitions in the grand band of  $^{124-128}\text{Ba}$  simultaneously, and the theoretical  $B(E2; I \rightarrow I-2)$  values peak at the neutron midshell also for  $I=4, 6,$  and  $8$  transitions for the Ba isotopes.

Recently, Próchniak *et al.* [47] performed a microscopic calculation of the low-lying quadrupole collective states of even-even nuclei from the region of  $50 < Z, N < 82$  within the framework of the general Bohr Hamiltonian (GBH) with no free parameters. They included the dynamical effects of the coupling with pairing vibrations and demonstrated that the effects are important for the description of the collective states. In our calculations the pairing vibrations have been considered through the couplings between a two-phonon  $0^+$  state and two-quasiparticle  $0^+$  states, and important effects as well as remarkable cancellation mechanism for the  $0^+$  couplings in connection with the three-body interaction have been discussed [18]. It should be noted here that the quadrupole-pairing interaction has been included as a symmetry restoring *residual* interaction and treated *dynamically* in our BET analysis [34,18,19].

The position of the present work may be considered in between the GCM analysis by Petkov *et al.* [12] and the GBH analysis by Próchniak *et al.* [47] in terms of the number of adjustable parameters. The fits to the experiment for  $^{124-132}\text{Ba}$  obtained by the GCM analysis [12] are considerably good for both the level schemes and most of the strong  $E2$  transitions, owing to the eight adjustable parameters. Looking at the results for  $^{122-136}\text{Ba}$  in the GBH calculation [47], the first  $2^+$  state seems too high and the energy scale of the theoretical spectra is too stretched except for a few nuclei in the midshell ( $N=66$ ) region, and such trend increases as going away from the midshell region. Considering the ab-

sence of free parameters, their  $B(E2; 2_1^+ \rightarrow 0_1^+)$  seems to reproduce correct tendency of increasing with decreasing neutron number down to the midshell, though there remain sensible discrepancies between the prediction and experiment for the midshell Ba isotopes.

Compared to the potentials derived by Petkov *et al.* for  $^{124-132}\text{Ba}$  (Fig. 2 in Ref. [12]), the potential minima  $\beta_{min}$  seem rather small in our cases. Also the prolate-oblate energy differences seem too small in our present results, which may relate to the problem of over bunching and staggering of levels in the quasi- $\gamma$  band. In Ref. [46], the problem of too prominent  $\gamma$  softness is remedied to a certain extent by adjusting artificially the position of the intruder proton  $h_{11/2}$  state in the way mentioned before. In the present analysis, however, such an artificial adjustment of the single-particle energy is not performed.

In the macroscopic-microscopic calculations of Ragnarsson *et al.* [48], there appear some barriers between oblate and prolate shapes, when passing through the  $\gamma$  degree of freedom for lighter isotopes of barium. The potential structure around  $\gamma=30^\circ$  that acts as a kind of potential barrier between oblate and prolate shapes in the lighter barium isotopes and its disappearance in  $^{128}\text{Ba}$  are also discussed by Petkov *et al.* [12]. The barriers increase the rigidity of the potential energy to the gamma deformation. In the present analysis, however, the microscopic Hamiltonian is expanded up to the fourth order in terms of the collective bosons, and the  $\gamma$  dependence of the potential surface is limited only up to the order of  $\beta^3 \cos 3\gamma$  accordingly. This may be one of the reasons for the present discrepancies between our calculated and experimental properties of the quasi- $\gamma$  levels. To improve the  $\gamma$  dependence of the potentials in the present type of analysis, further investigations based on a much higher-order boson expansion are advisable.

The deformation energies obtained by Ragnarsson *et al.* [48] are much smaller than that of the present paper. A set of solutions with smaller deformation energies (e.g., about 2 MeV for  $^{126}\text{Ba}$ ) are also obtained in our previous calculation [18], which is due to the weaker interaction strengths  $f_2$  and  $g_2$  adopted with the use of smaller pairing gap energies derived from the experimental nuclear binding energies available at that time [49–52]. In the present analysis, however, a different set of solutions with larger deformation energies (e.g., about 6 MeV for  $^{126}\text{Ba}$ ) are obtained resulting from the use of slightly larger interaction strengths, which are required when we adopt slightly larger pairing gap energies estimated from the recent compilation of experimental nuclear binding energies [35]. Relatively larger deformation energies are also obtained in the GCM analysis by Petkov *et al.* (e.g., about 5.2 MeV for  $^{126}\text{Ba}$ ), where a good description of the ground-state and  $\gamma$  bands is obtained by varying freely the eight parameters in their GCM Hamiltonian. For  $^{124-128}\text{Ba}$ , the deformation energies in the present microscopic calculation are rather comparable with that of the GCM potentials, while for heavier isotopes our potentials are more shallow.

Finally we will make a brief comment on the structure of the  $0_2^+$  state. In the GCM calculations, the most dominant

component in the  $0_2^+$  state of  $^{128}\text{Ba}$  was shown to be the state with phonon triplets coupled to  $L=0$  (Fig. 7 in Ref. [12]). Also in our present analysis, the main component of the  $0_2^+$  state of  $^{128}\text{Ba}$  appears to be the three-phonon state, and the two-phonon component is rather dominant in the  $0_3^+$  state. Detailed investigation on the structure of the boson wave functions for the low-lying collective states and the  $0_2^+$  band based on the BET analysis will be reported elsewhere.

## V. CONCLUSIONS

The low-lying quadrupole collective states of midshell Ba isotopes are studied by means of the boson expansion theory. The original fermion Hamiltonian of the present model includes higher-order (many-body) terms of the  $QQ$  interaction to ensure the nuclear self-consistency in higher-order accuracy, and the quadrupole-pairing interaction to ensure the local Galilean invariance of the system. The microscopic boson image of the Hamiltonian and that of the  $E2$  operator

are constructed by using the normal-ordered linked-cluster expansion of the modified Marumori boson mapping. Numerical calculations are performed by using the techniques developed by Kishimoto and Tamura [14,15] with several refinements developed in Refs. [17–19].

It is shown that the marked increase of quadrupole collectivity, indicated by the enhancement of experimental  $B(E2)$ , as neutron numbers approach the midshell value of  $N=66$  can be reproduced naturally in terms of the microscopic BET by using a rather standard value of the effective charge.

## ACKNOWLEDGMENTS

The author is grateful to K. Uchiyama for many critical discussions on experimental data. Thanks are also due to Dr. K. Matsuyanagi for helpful comments. This research was supported in part by the Grant-in-Aid of the Ministry of Education, Science, Sports and Culture under Contract No. 09740195.

- 
- [1] S. Raman, J.A. Sheikh, and K.H. Bhatt, Phys. Rev. C **52**, 1380 (1995).
- [2] T. Otsuka, X.-W. Pan, and A. Arima, Phys. Lett. B **247**, 191 (1990).
- [3] J.C. Walpe, B.F. Davis, S. Naguleswaran, W. Reviol, U. Garg, X.-W. Pan, D.H. Feng, and J.X. Saladin, Phys. Rev. C **52**, 1792 (1995).
- [4] T. Morikawa, M. Oshima, T. Sekine, Y. Hatsukawa, S. Ichikawa, H. Iimura, A. Osa, M. Shibata, and A. Taniguchi, Phys. Rev. C **46**, R6 (1992).
- [5] K. Uchiyama, K. Furuno, T. Shizuma, M. Sugita, M. Kato, Y. Tokita, M. Murasaki, N. Hashimoto, H. Takahashi, T. Komatsubara, K. Matsuura, T. Tanaka, and Y. Sasaki, Eur. Phys. J. A **2**, 13 (1998).
- [6] A. Dewald, D. Weil, R. Krücken, R. Kühn, R. Peusquens, H. Tiesler, O. Vogel, K.O. Zell, P. von Brentano, D. Bazzacco, C. Rossi-Alvarez, P. Pavan, D. De Acuña, G. De Angelis, and M. De Poli, Phys. Rev. C **54**, R2119 (1996).
- [7] P. Petkov, S. Harissopulos, A. Dewald, M. Stolzenwald, G. Böhm, P. Sala, K. Schiffer, A. Gelberg, K.O. Zell, P. von Brentano, and W. Andrejtscheff, Nucl. Phys. **A543**, 589 (1992).
- [8] O. Stuch, K. Jessen, R.S. Chakrawarthy, A. Dewald, R. Kühn, R. Krücken, P. Petkov, R. Peusquens, H. Tiesler, D. Weil, I. Wiedenhöver, K.O. Zell, P. von Brentano, C. Ender, T. Härtlein, F. Köck, O. Koschorrek, and P. Reiter, Phys. Rev. C **61**, 044325 (2000).
- [9] S.M. Burnett, A.M. Baxter, S. Hinds, F. Pribac, R.H. Spear, and W.J. Vermeer, Nucl. Phys. **A432**, 514 (1985).
- [10] S.M. Burnett, A.M. Baxter, G.J. Gyapong, M.P. Fewell, and R.H. Spear, Nucl. Phys. **A494**, 102 (1989).
- [11] P.J. Rothschild, A.M. Baxter, S.M. Burnett, M.P. Fewell, G.J. Gyapong, and R.H. Spear, Phys. Rev. C **34**, 732 (1986).
- [12] P. Petkov, A. Dewald, and W. Andrejtscheff, Phys. Rev. C **51**, 2511 (1995).
- [13] K. Schiffer, S. Harissopulos, A. Dewald, A. Gelberg, K.O. Zell, P. von Brentano, P.J. Nolan, A. Kirwant, D.J.G. Love, D.J. Thornley, and P.J. Bishop, J. Phys. G **15**, L85 (1989).
- [14] T. Kishimoto and T. Tamura, Nucl. Phys. **A192**, 246 (1972).
- [15] T. Kishimoto and T. Tamura, Nucl. Phys. **A270**, 317 (1976).
- [16] T. Kishimoto and T. Tamura, Phys. Rev. C **27**, 341 (1983).
- [17] H. Sakamoto and T. Kishimoto, Nucl. Phys. **A486**, 1 (1988).
- [18] H. Sakamoto and T. Kishimoto, Nucl. Phys. **A528**, 73 (1991).
- [19] H. Sakamoto, Phys. Rev. C **52**, 177 (1995).
- [20] S.G. Nilsson, C.F. Tsang, A. Sobiczewski, Z. Szymański, S. Wycech, C. Gustafson, I.-L. Lamm, P. Möller, and B. Nilsson, Nucl. Phys. **A131**, 1 (1969).
- [21] T. Bengtsson and I. Ragnarsson, Nucl. Phys. **A436**, 14 (1985).
- [22] T. Seo, Z. Phys. A **324**, 43 (1986).
- [23] B.R. Mottelson, preprint, NORDITA pub.288, 1967.
- [24] T. Kishimoto, J.M. Moss, D.H. Youngblood, J.D. Bronson, C.M. Rozsa, D.R. Brown, and A.D. Bacher, Phys. Rev. Lett. **35**, 552 (1975).
- [25] T. Kishimoto, in *Proceedings of the International Conference on Highly Excited States in Nuclear Reactions*, Osaka, 1980, edited by H. Ikegami and M. Muraoka (RCNP, Osaka, 1980), p. 377.
- [26] T. Kishimoto, T. Tamura, and T. Kammuri, Prog. Theor. Phys. Suppl. **74&75**, 170 (1983).
- [27] H. Sakamoto and T. Kishimoto, Nucl. Phys. **A501**, 205 (1989); **A501**, 242 (1989).
- [28] E.R. Marshalek, Phys. Rev. Lett. **51**, 1534 (1983); Phys. Rev. C **29**, 640 (1984); Phys. Lett. B **244**, 1 (1990).
- [29] M. Matsuo and K. Matsuyanagi, Prog. Theor. Phys. **78**, 591 (1987).
- [30] S.A. Stotts and T. Tamura, Phys. Rev. C **40**, 2342 (1989).
- [31] H. Aiba, Prog. Theor. Phys. **84**, 908 (1990).
- [32] K. Yamada, Prog. Theor. Phys. **89**, 995 (1993).
- [33] S. T. Belyaev, Yad. Fiz. **4**, 936 (1966) [Sov. J. Nucl. Phys. **4**, 671 (1967)].
- [34] H. Sakamoto and T. Kishimoto, Phys. Lett. B **245**, 321 (1990).
- [35] G. Audi and A.H. Wapstra, Nucl. Phys. **A595**, 409 (1995).
- [36] H. Feshbach, Ann. Phys. (N.Y.) **5**, 357 (1958); **19**, 287 (1962).

- [37] S. Okubo, Prog. Theor. Phys. **12**, 603 (1954).
- [38] N. Fukuda, K. Sawada, and M. Taketani, Prog. Theor. Phys. **12**, 156 (1954).
- [39] A. Messiah, *Quantum Mechanics* (North-Holland, Amsterdam, 1961), Vol. II, Chap. XVI.
- [40] K. Suzuki and R. Okamoto, Prog. Theor. Phys. **71**, 1221 (1984).
- [41] A. Bohr, Mat. Fys. Medd. K. Dan. Vidensk. Selsk. **6**, 14 (1952).
- [42] A. Bohr and B.R. Mottelson, Mat. Fys. Medd. K. Dan. Vidensk. Selsk. **27**, 6 (1953).
- [43] K. Pomorski, T. Kaniowska, A. Sobiczewski, and S.G. Rohoziński, Nucl. Phys. **A283**, 394 (1977).
- [44] T. Kubo, H. Sakamoto, T. Kammuri, and T. Kishimoto, Phys. Rev. C **54**, 2331 (1996).
- [45] J.M. Eisenberg and W. Greiner, *Nuclear Theory* (North-Holland, Amsterdam, 1972), Vol. 3, Chap. 10.
- [46] T. Komatsubara, T. Hosoda, H. Sakamoto, T. Aoki, and K. Furuno, Nucl. Phys. **A496**, 605 (1989).
- [47] L. Próchniak, K. Zając, K. Pomorski, S.G. Rohoziński, and J. Srebrny, Nucl. Phys. **A648**, 181 (1999).
- [48] I. Ragnarsson, A. Sobiczewski, R.K. Sheline, S.E. Larsson, and B. Nerlo-Pomorska, Nucl. Phys. **A233**, 329 (1974).
- [49] A.H. Wapstra and N. Gove, Nucl. Data Tables **9**, 265 (1971).
- [50] A.H. Wapstra and K. Bos, At. Data Nucl. Data Tables **19**, 177 (1977).
- [51] P. Möller and J.R. Nix, At. Data Nucl. Data Tables **26**, 165 (1981).
- [52] A. H. Wapstra and G. Audi, Nucl. Phys. **A432**, 1 (1985).